InGaN-based light-emitting diodes grown and fabricated on nanopatterned Si substrates

Dongmei Deng,[1,a)] Naisen Yu,[1] Yong Wang,[1] Xinbo Zou,[1] Hao-Chung Kuo,[2] Peng Chen,[1] and Kei May Lau[1,a)]
[1]*Department of Electronic and Computer Engineering, Photonics Technology Center, Hong Kong University of Science and Technology, Clear Water Bay, Kowloon, Hong Kong 00852*
[2]*Institute of Electro-Optical Engineering, National Chiao Tung University, Hsinchu 300, Taiwan*

(Received 13 November 2009; accepted 18 April 2010; published online 18 May 2010)

InGaN-based light-emitting diodes (LEDs) were grown and fabricated on nanoscale patterned Si (111) substrates (NPSi). Using anodized aluminum oxide as the etch mask, the NPSi was prepared with an average nanopore diameter of 150 nm and interpore distance of 120 nm. LEDs grown on NPSi exhibit relaxed tensile stress relative to the ones grown on microscale patterned Si (111) substrates (MPSi). Nanoheteroepitaxial lateral overgrowth was significantly promoted on NPSi, which led to extensive dislocation bending and annihilation. The devices made on NPSi exhibit lower leakage current and higher light output power as compared with those on MPSi. © *2010 American Institute of Physics*. [doi:10.1063/1.3427438]

GaN-based materials have been studied extensively for various applications in visible to ultraviolet range of the optical spectrum. Si substrate, with a lower manufacturing cost and a better thermal conductivity as compared to the sapphire substrate, is considered as a promising candidate for the growth of GaN-based devices. However, due to the large lattice and thermal mismatch, heteroepitaxy of GaN on Si usually results in high-density of defects and residual strain,[1–4] which in turn degrade both the electrical and optical performance of devices.

Although the epitaxial lateral overgrowth (ELO) technique alleviates these problems to a certain extent,[5,6] the quality of GaN-based films grown on Si is still not comparable to those obtained on conventional substrates like sapphire and SiC.[6,7] The typical dislocation density in GaN grown on Si is $10^9-10^{11}/\mathrm{cm}^2$.[1,8] Both theoretical and experimental studies have suggested that it is possible to further reduce the defect density when the ELO approach is extended to the nanoscale.[9–11] Light-emitting diode (LED) structures grown on nanoscale patterned sapphire substrates already showed a reduced dislocation density and an increased output power.[12]

Previously, we reported LED grown on microscale ($340\times340\ \mu\mathrm{m}^2$) grid-patterned Si substrate (MPSi for short in later discussion) with SiN_x as an *in situ* nanomask.[13] Results indicated that the SiN_x nanomask is effective on improving crystal quality and releasing the tensile stress. However, since SiN_x is grown *in situ*, it is difficult to control the thickness and the surface morphology of SiN_x. Consequently it is challenging to guarantee the crystalline quality of LED structures. Therefore, nanoscale patterned Si substrate (NPSi) has been proposed with the size and shape of mask under control. By using the NPSi substrate, the nanoscale ELO will be achieved, and GaN islands with small size and distance will achieve fast and uniform coalescence. In comparison, in the microscale ELO, a thick epilayer, typically $1-1.5\ \mu\mathrm{m}$,[14] needs to be grown to get full coalescence.

Although some preliminary work of GaN grown on NPSi were conducted and signs of reduction in dislocation density and improvement of tensile stress were shown,[15–18] most of them used exotic materials as nanomask. The use of nanomask tends to introduce impurity contamination and increase manufacturing cost. Other common techniques for fabricating the nanopattern, including E-beam lithography and nanoimprint lithography are usually low throughput and high cost. In this study, self-ordered anodized aluminum oxide (AAO) technique,[19] together with inductively coupled plasma (ICP) etching were used for fabricating NPSi. It is a simple, fast, and low-cost technique. The diameter, depth, and distance of nanoholes can be easily controlled for optimized growth.

The NPSi was prepared by the AAO process and ICP technique on a 2 in. Si (111) wafer. The anodization was performed at 6 °C in 0.3 M phosphoric acid under an applied voltage of 120 V. After anodization for 30 min, self-assembled AAO nanoarrays were uniformly distributed on the Si surface. By ICP etching, the AAO pattern was transferred to the Si substrate. The AAO mask was then removed by wet etching. The top-view scanning electron microscope (SEM) image in Fig. 1(a) shows the NPSi after removing the AAO mask. Nanopore arrays were uniformly distributed on the entire 2 in. Si substrate with an average nanopore diameter of ~150 nm, interpore distance of ~120 nm, and an etched depth of ~250 nm. LED structures were grown by metal-organic chemical vapor deposition in an Aixtron 2000 HT system. For comparison, the same LED structures were also grown on the MPSi ($340\times340\ \mu\mathrm{m}^2$ grid-pattern separated by 20 μm trenches). Detailed substrate preparation and growth procedure for LED on MPSi were reported elsewhere.[13] For the growth on NPSi, prior to the deposition, substrates were heated up to 1170 °C for 10 min under H_2 ambient to remove the native oxide on the surfaces. Then, an AlN nucleation layer (~40 nm) was deposited, followed by the growth of a 200 nm thick AlGaN buffer layer and an 800 nm thick undoped GaN. Before the growth of a 1 μm thick Si doped GaN layer for contact, the 250 nm AlGaN/AlN interlayer which aimed to decrease the tensile stress was inserted. Five stacks of InGaN/GaN multiple quantum wells

[a)]Authors to whom correspondence should be addressed. Electronic addresses: dmdeng@ust.hk and eekmlau@ust.hk. Tel.: 852-23588843 and 852-23587049.

 © 2010 American Institute of Physics

Downloaded 10 Dec 2010 to 143.89.47.110. Redistribution subject to AIP license or copyright; see http://apl.aip.org/about/rights_and_permissions

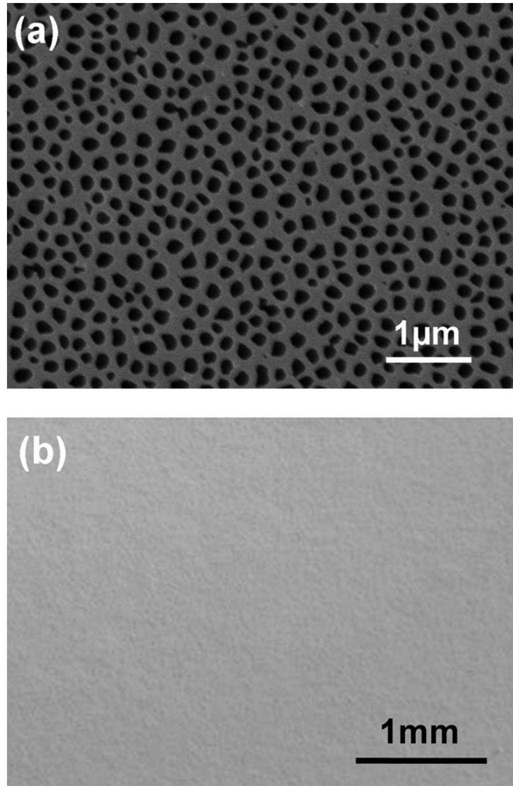

FIG. 1. (a) The top-view SEM image of the NPSi. (b) The optical microscopy image of the surface of LED grown on NPSi.

(MQWs) with well thickness of 2.6 nm and barrier thickness of 10 nm were grown as the active layer, and on top of MQWs, a 150 nm thick Mg doped p-GaN layer was deposited. After growth, the sample surface was examined under optical microscopy [Fig. 1(b)]. No crack could be observed on the whole wafer, and the surface was mirrorlike.

For cross-sectional transmission electron microscopy (TEM) studies, both MPSi and NPSi samples were prepared using conventional mechanical thinning followed by ion beam milling. All TEM analyses were carried out on a JEOL 2010F field-emission microscope operating at 200 keV. Figures 2(a) and 2(b) show the full phase view of LED structures imaged using multibeam bright-field diffraction condition near the $\langle 1\bar{1}00\rangle$ zone axis. Although threading dislocations (TDs) were visible in both types of samples, fewer dislocations were observed in the NPSi sample [Fig. 2(b)] and fewer dislocations extend to the MQWs region as compared to the MPSi sample [Fig. 2(a)]. Figures 2(c) and 2(d) are TEM images taken from the interface of the epilayer/NPSi in the same region but under different diffraction conditions. Figure 2(c) was collected under multibeam dark-field diffraction condition near $\langle 1\bar{1}00\rangle$ zone axis while Fig. 2(d) used a two-beam dark-field under $g=\langle 0002\rangle$. Careful comparison of Fig. 2(c) and 2(d) indicates that several dislocations disappeared when $g=\langle 0002\rangle$. It suggests that most dislocations had a Burger's vector of $\langle 11\bar{2}0\rangle/3$ thus they were "a-type" dislocations. Moreover, it is obvious that most of the TDs were restricted in the AlGaN layer. Some dislocations changed their directions by bending at the AlGaN/GaN interface, while some dislocations annihilated or bent inside the AlGaN buffer layer directly over the holes. As a result, the density of TDs at the top surface was much lower.

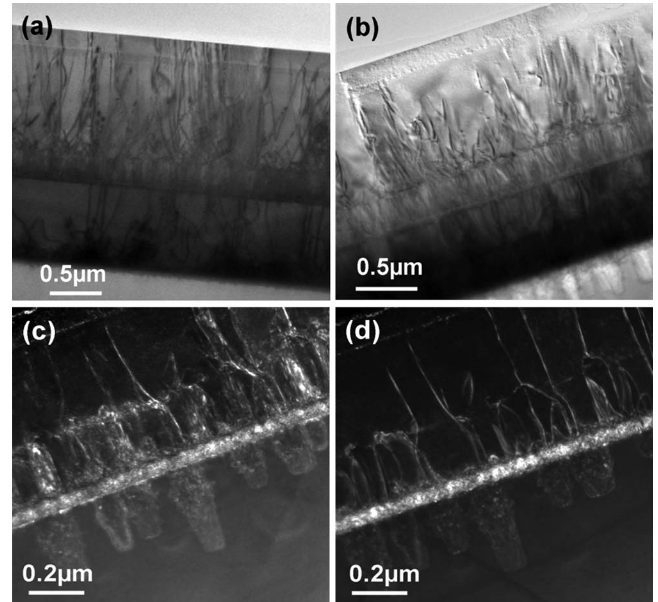

FIG. 2. Bright-field images of LEDs grown on MPSi (a) and NPSi (b), (c) Multibeam dark-field images collected near zone axis. (d) Two-beam dark-field images collected using $g=\langle 0002\rangle$. Note that (c) and (d) are collected at the same region.

To investigate the residual strain in the GaN films, Raman backscattering measurements were performed at room temperature. Figure 3 compares the Raman spectra of the LEDs on NPSi and on MPSi. It was reported that the Raman shift of E_2(High) in stress-free GaN layer is around 567.2 cm^{-1}.[20] The E_2(High) shift is 565.4 cm^{-1} and 564.5 cm^{-1}, for samples on NPSi and on MPSi, respectively. The deviation of the E_2(High) peaks from the intrinsic position indicates the release of residual tensile stress. For GaN, the E_2(high) mode shifts linearly with stress in 2.9 cm^{-1}/GPa for biaxial stress. The estimated tensile stress in NPSi and MPSi are 0.62 GPa and 0.93 GPa, respectively. It is obvious that the LED grown on NPSi has less tensile strained than that on MPSi, although both *in situ* SiN_x and selective area growth technique were used during the growth of LED on MPSi. The stress difference is possibly due to the fact that when the patterns were in nanoscale, the initially formed GaN islands had relatively small size and narrow spacing. This would lead to a faster coalescence, and the coalescence boundary could facilitate the stress release.

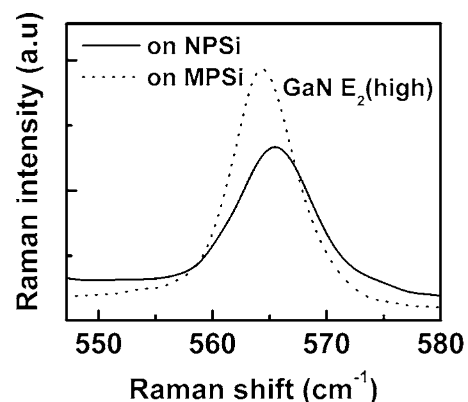

FIG. 3. Raman spectra of LEDs grown on NPSi and MPSi under $z(xx)z^{-}$ back scattering geometry.

Downloaded 10 Dec 2010 to 143.89.47.110. Redistribution subject to AIP license or copyright; see http://apl.aip.org/about/rights_and_permissions

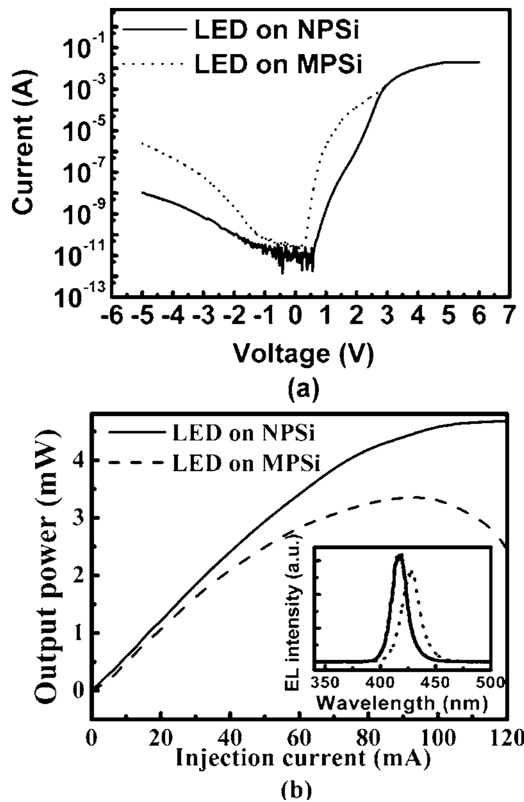

FIG. 4. (a) The I-V characteristics. (b) The L-I curves. The inset is the comparison of EL spectra at 20 mA injection current.

LED chips of 300×300 μm^2 were fabricated on both NPSi and MPSi. Figure 4(a) shows the room temperature current-voltage (I-V) characteristics of these two samples. Both types of LEDs exhibited a forward voltage of ~4.7 V at 20 mA. The LEDs on NPSi exhibited a much lower leakage current as compared to those on MPSi. This suggests that the density of TDs of the epitaxial film was reduced by using the NPSi. For the light output power measurement, the fabricated LED devices were mounted onto TO-5 cans. An integrating sphere was used for collecting all the light emitted by the LED and directing the light to a charge-coupled device detector. During the measurement, a Tektronix PS2520G programmable power supply was used to provide the biasing current. The current dependent output power (L-I) curves of these two unpackaged LED samples are shown in Fig. 4(b). At the injection current of 20 mA, the output power of the LED on NPSi was 1.28 mW, 21% higher than that on MPSi. It should be noted that a slight portion of the power improvement may come from the 10 nm wavelength difference.[21] Moreover, the output power of the LED on MPSi saturated at an injection current of ~90 mA, while the output power of the LED on NPSi saturated at a higher current of ~110 mA. The reduction in output power under high injection currents on the MPSi sample has been suggested to be related to TDs.[22] At high injection, phonon-assisted transport of holes via tunneling at defect sites along dislocation takes place, leading to an enhanced nonradiative parasitic process, thus, the output power is weakened. This is in good agreement with our observations in TEM. The inset of Fig. 4(b) shows the electroluminescence (EL) spectra of LEDs on NPSi and on MPSi at 20 mA injection current. An increase in intensity and a blueshift of the peak wavelength are noted on the NPSi sample as compared with the MPSi one. In combination with the Raman results, the blueshift of the LED on NPSi is considered as a sign of strain-release in the film grown on NPSi.

In summary, crack-free InGaN based LED structures were grown and fabricated on NPSi. The material showed good surface morphology, reduced tensile strain, and lower dislocation density. The LEDs grown on NPSi exhibited a higher output power at 20 mA and a lower leakage current as compared with LEDs on conventional MPSi. These results suggest the feasibility of using NPSi for the growth of high power LEDs on Si substrates.

The authors wish to thank Tze Kin Cheung and Ching-Hsueh Chiu for useful discussions on this work. The research work was supported in part by a grant (Grant No. 615705) from the Research Grants Council and a grant (Grant No. GHP/034/07GD) from the Innovation and Technology Commission (ITC) of Hong Kong Special Administrative Government (HKSAR).

[1] A. Dadgar, M. Poschenrieder, J. Bläsing, K. Fehse, A. Diez, and A. Krost, Appl. Phys. Lett. **80**, 3670 (2002).
[2] S. A. Nikishin, N. N. Faleev, V. G. Antipov, S. Fancoeur, L. Grave de Peralta, G. A. Seryogin, H. Temkin, T. I. Prokofyeve, M. Holtz, and S. N. G. Chu, Appl. Phys. Lett. **75**, 2073 (1999).
[3] H. Yu, M. K. Ozturk, S. Ozcelik, and E. Ozbay, J. Cryst. Growth **293**, 273 (2006).
[4] S. Tanaka, Y. Honda, N. Sawaki, and M. Hibino, Appl. Phys. Lett. **79**, 955 (2001).
[5] E. Feltin, B. Beaumont, P. Vennéguès, M. Vaille, P. Gibart, T. Riemann, J. Christen, L. Dobos, and B. Pécz, J. Appl. Phys. **93**, 182 (2003).
[6] M. Yamada, T. Mitani, Y. Narukawa, S. Shioji, I. Niki, S. Sonobe, K. Deguchi, M. Sano, and T. Mukai, Jpn. J. Appl. Phys., Part 2 **41**, L1431 (2002).
[7] O. H. Nam, M. D. Bremser, B. L. Ward, R. J. Nemanich, and R. F. Davis, Jpn. J. Appl. Phys., Part 2 **36**, L532 (1997).
[8] A. Dadgar, M. Poschenrieder, J. Bläsing, O. Contreras, F. Bertram, T. Riemann, A. Reiher, M. Kunze, I. Daumiller, A. Krtschil, A. Diez, A. Kaluza, A. Modlich, M. Kamp, J. Christen, F. A. Ponce, E. Kohn, and A. Krost, J. Cryst. Growth **248**, 556 (2003).
[9] S. D. Hersee, D. Zubia, X. Sun, R. Bommena, M. Fairchild, S. Zhang, D. Burckel, A. Frauenglass, and S. R. J. Brueck, IEEE J. Quantum Electron. **38**, 1017 (2002).
[10] D. Zubia, S. H. Zaidi, S. D. Hersee, and S. R. J. Bruech, J. Vac. Sci. Technol. B **18**, 3514 (2000).
[11] D. Zubia and S. D. Hersee, J. Appl. Phys. **85**, 6492 (1999).
[12] C. H. Chan, C. H. Hou, S. Z. Tseng, T. J. Chen, H. T. Chien, F. L. Hsiao, C. C. Lee, Y. L. Tsai, and C. C. Chen, Appl. Phys. Lett. **95**, 011110 (2009).
[13] B. Zhang, H. Liang, Y. Wang, Z. Feng, K. W. Ng, and K. M. Lau, J. Cryst. Growth **298**, 725 (2007).
[14] L. Macht, P. R. Hageman, S. Haffouz, and P. K. Larsen, Appl. Phys. Lett. **87**, 131904 (2005).
[15] K. Y. Zang, S. J. Chua, J. H. Teng, N. S. S. Ang, A. M. Yong, and S. Y. Chow, Appl. Phys. Lett. **92**, 243126 (2008).
[16] K. Y. Zang, Y. D. Wang, S. J. Chua, and L. S. Wang, Appl. Phys. Lett. **87**, 193106 (2005).
[17] A. Y. Polyakov, A. V. Markov, M. V. Mezhennyi, A. V. Govorkov, V. F. Pavlov, N. B. Smirnov, A. A. Donskov, L. I. D'yakonov, Y. P. Kozlova, S. S. Malakhov, T. G. Yugova, V. I. Osinsky, G. G. Gorokh, N. N. Lyahova, V. B. Mityukhlyaev, and S. J. Pearton, Appl. Phys. Lett. **94**, 022114 (2009).
[18] J. Liang, S. K. Hong, N. Kouklin, R. Beresford, and J. M. Xu, Appl. Phys. Lett. **83**, 1752 (2003).
[19] H. Masuda, H. Yamada, M. Satoh, H. Asoh, M. Nakao, and T. Tamamura, Appl. Phys. Lett. **71**, 2770 (1997).
[20] F. Demangeot, J. Frandon, M. A. Renucci, O. Briot, B. Gil, and R. L. Aulumbard, Solid State Commun. **100**, 207 (1996).
[21] A. Y. Kim, W. Götz, D. A. Steigerwald, J. J. Wierer, N. F. Gardner, J. Sun, S. A. Stockman, P. S. Martin, M. R. Krames, R. S. Kern, and F. M. Steranka, Phys. Status Solidi A **188**, 15 (2001).
[22] B. Monemar and B. E. Sernelius, Appl. Phys. Lett. **91**, 181103 (2007).

Downloaded 10 Dec 2010 to 143.89.47.110. Redistribution subject to AIP license or copyright; see http://apl.aip.org/about/rights_and_permissions